energies

Article

Forces and Stresses in the Windings of a Superconducting Fault Current Limiter

Janusz Kozak

Faculty of Engineering and Computer Science, Department of Electrical Engineering and Electrotechnology, Lublin University of Technology, 38A Nadbystrzycka St., 20-618 Lublin, Poland; j.kozak@pollub.pl

Abstract: This paper presents the design of a Superconducting Fault Current Limiter (SFCL) and calculation results of forces and stresses in the windings of a resistive fault current limiter. The design of the fault current limiter consists of two parallelly connected and magnetically coupled windings, cooled by a single stage cryocooler. Magnetically compensated windings made of HTS tape give a very low voltage on the limiter at a nominal current. Limitation of the short-circuit time and the value of the maximum initial fault current reduces the thermal and dynamic effects of the passage of a fault current. Using devices which limit the value of a fault current can lower the level of required short-circuit capacity of the elements in a system. However, selected means of fault currents limitation must maintain the power quality standards. A perfect fault current limiter is required to have substantial impedance in fault conditions and zero impedance at work currents. Such requirements are met by a SFCL. An increase of current caused by the occurrence of a fault current results in the transition of the superconducting material from the superconducting state into the resistive state. This increases the impedance of short-circuit loop, allowing the fault current value to decrease. During a short-circuit, the forces generated from the short-circuit current also act on the limiter windings. Short-circuit current causes stresses in the superconducting tape. Exceeding the permissible stress value results in an irreversible reduction in the critical current of the superconducting tape. Calculations of the forces and stresses in the HTS tape for the maximum value of the short-circuit current were carried out using the finite element method. The constructed limiter was tested and the winding design ensures that the tape stresses are at a safe level even for short-circuit currents.

Keywords: fault current limiter; superconducting tape; short-circuit

Citation: Kozak, J. Forces and Stresses in the Windings of a Superconducting Fault Current Limiter. *Energies* **2022**, *15*, 6519. https://doi.org/10.3390/en15186519

Academic Editor: Adam Smoliński

Received: 31 July 2022
Accepted: 2 September 2022
Published: 7 September 2022

1. Introduction

Limitation of the duration of a short-circuit time and the value of the maximum initial fault current reduce the thermal and dynamic effects of the passage of a fault current. Using devices which limit the value of a fault current can lower the level of required short-circuit capacity of the elements in a system. However, selected means of fault currents limitation must maintain the power quality standards. A perfect fault current limiter is required to have substantial impedance in fault conditions and zero impedance at work currents. Such requirements are met by a Superconducting Fault Current Limiter (SFCL). An increase of current caused by the occurrence of a fault current results in the transition of the superconducting material from the superconducting state into the resistive state. This increases the impedance of a short-circuit loop, allowing the fault current value to decrease. Numerous papers concentrate on the subject of inductive type fault current limiters [1–19], limiters with saturated core [20–22], resistive SFCLs [23], flux coupling SFCLs [24], transformer type SFCLs [25], comparisons of various types of SFCLs [26–28], integration of SFCLs in a power grid [29–32], and fault detection and analysis [33–37]. Magnetic core limiters are large and very heavy. In inductive limiters with copper windings, there is an undesirable voltage drop for the operating current. In bifilar resistive limiters built for medium voltages, there are a large number of connections between modules. Each design has its ad-vantages and disadvantages. The presented design is lightweight, the voltage drop for operating currents is very low, and the number of connections is reduced to a minimum of two connections to current feedthroughs. The disadvantage of this design is the development of forces acting on the limiter windings and the development of stresses in the superconducting tape. The forces acting on the HTS tape depend on the value of the current in the tape and the value of the magnetic induction. The magnetic flux density depends on the value of the current, the dimensions of the windings and the number of windings. An appropriate winding design ensures safe operation of the limiter, where the stresses in the HTS tape are less than the maximum stresses. The exact value of the short-circuit current obtained from the measurements made it possible to precisely determine the stresses in the HTS tape for the presented design.

2. The Design of the Limiter

2.1. Concept

The concept of a resistive SFCL cooled by a cryocooler has been chosen to simplify the cooling system and reduce the necessary maintenance. This is a compact and light design that requires only electric power to operate. The lack of liquid nitrogen or external reactors makes such a design a desired smart grid element. Its small size and conduction cooling design enable the limiter to be installed next to a circuit braker inside a substation (Figure 1). The main parameters of the SFCL are presented in Table 1.

Figure 1. Resistive superconducting fault current limiter (SFCL).

Table 1. Parameters of the SFCL.

Parameter		Value
Nominal voltage	U_N	6 kV
Nominal current	I_N	140 A
Overload current	$I_{Overload}$	420 A
Voltage on the limiter @ I_N	U_{SCFL}	0.2 V
Voltage on the limiter @ $I_{Overload}$	$U_{SCFL}O_{verload}$	0.6 V
Prospective peak current	i_{peak}	81 kA
First peak limiting	i_p	1.9 kA
Limitation time	t_{lim}	80 ms
Response time of the surge current limitation	$t_{response}$	0.6 ms
Operating temperature	T	72 K
Cryostat height	H	1 m
Cryostat diameter	$O.D.$	0.87 m
Weight	m	340 kg

2.2. Cryogenic System

The presented design is a superconducting fault current limiter cooled by a single stage cryocooler (Figure 2).

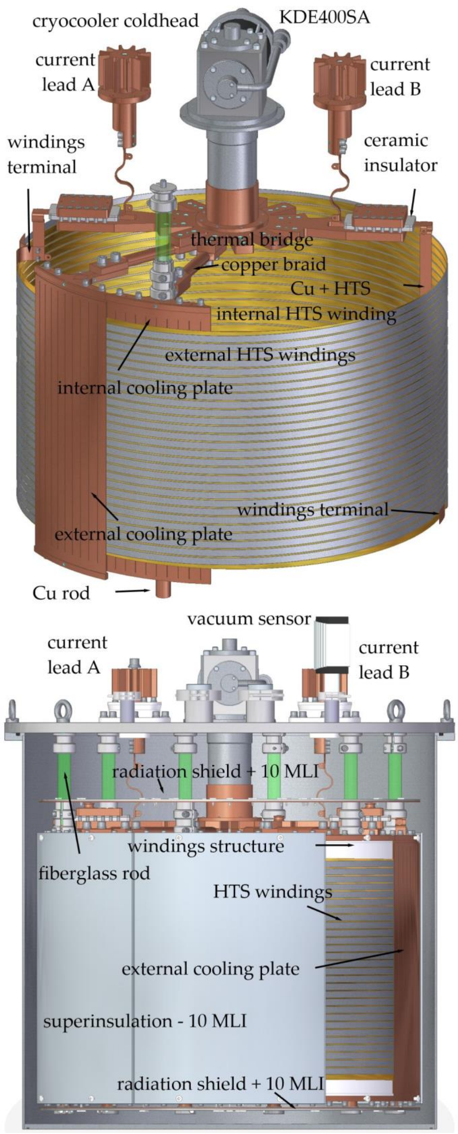

Figure 2. HTS windings construction and cross-section of SFCL [38].

The device consists of two superconducting windings (28.5 turns each), cooled by a KDE400SA coldhead. The cryocooler head removes the heat reaching the interior of the cryostat through radiation and thermal conduction, as well as the heat from the superconducting windings generated from AC losses and Joule losses (which result from current flow through the current leads). Assuming good vacuum insulation of 10^{-6} mbar, convection losses are negligible. Total losses calculated at nominal current are 37.5 W. The power capacity of the cryocooler is more than 130 W at 72 K, which assures a stable temperature of the superconductor during overload current passage.

2.3. Numerical Calculation

The design of the windings has been evaluated using a numerical model. The voltage on the limiter and the temperature evolution during the current limiting process were calculated taking into account properties of HTS tape, copper and fibreglass in a wide range of temperatures. [39]. Numerical calculations determined the maximum short circuit time to avoid overheating of the superconducting windings.

2.4. Design

The HTS windings, which carry current in reverse directions, are connected in parallel. The radial forces affecting the windings during a short-circuit were limited by a special construction of the superconducting windings which are wound in opposite direction. Such a design provides good magnetic coupling and low leakage reactance. The HTS tape was insulated with fiberglass. The terminals of the windings are situated on the inside of the windings structure to allow the outside of the windings be covered with the multilayer insulation and to protect the terminals from mechanical damage during assembly and cryostating. The exterior of the windings structure was covered with 10 layers of superinsulation (Figure 3). The multilayer insulation (MLI) covering the superconducting windings reduces heat transfer from the cryostat walls to the windings.

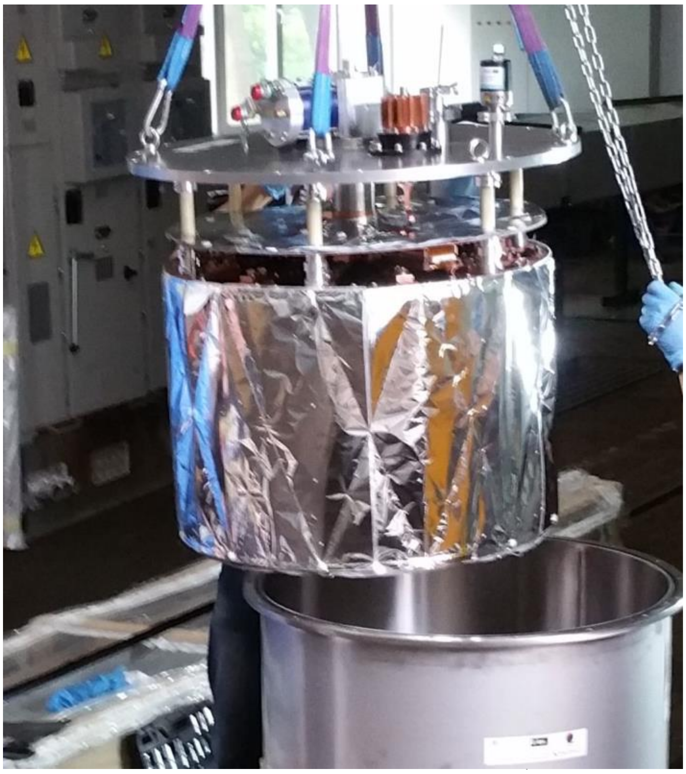

Figure 3. Superconducting fault current limiter assembly in a cryostat [38].

The HTS windings were connected to copper current leads and cooled through AL_2O_3 ceramic insulators. Each of the windings has copper terminals soldered to the HTS tape. The copper terminals are bolted to the current leads (Figure 2). Except for two joints between coils ends and the current leads, there are no coil interconnections which could add unwanted resistance inside the cooled coils. The design assumes contact cooling of the current leads. The heat generated in the cryostat (mainly by the current leads) should be less than the cooling capacity of the cryocooler. The heat flow throw the current leads and the Joule losses at the nominal current and overload current were calculated [38]. Heat loss per one current lead is below 14 W at rated current and about 19 W at 420 A. The electrical diagram of the SFCL consists of two windings connected in parallel. The internal winding is wound clockwise, while the external winding is wound anticlockwise. Between the windings there is a thin layer of fiberglass, which provides insulation and mechanical strength for the windings.

2.5. Manufacturing

The windings made of SF12100 (Ic = 300 A) tape were wound onto a fiberglass structure. Each of the HTS tapes of the superconducting windings is 66 m long. To assure good temperature distribution during cooling and fast re-cooling after a fault current limitation, the fiberglass structure of the superconducting windings includes an internal and an external copper cooling plate. The copper plates incised into vertical stripes reduce the eddy currents losses and ensure good conduction cooling of the windings. Such a design makes the SFCL simple in structure, as well as reliable and easy to manufacture. Additional 12 copper rods installed inside the windings improve heat conduction and reduce the temperature difference between the upper and the lower side of the windings. In order to lower the heat transfer, the construction of the windings is suspended under cryostat lid on six fiberglass rods.

3. Test Setup

A short-circuit test was performed in the accredited Switchgear and Controlgear Testing Laboratory of Electrotechnical Institute in Warsaw. The test circuit (Scheme 1) consisted of 2500 MVA short-circuit generator—G (Figure 4), master breaker—MB, making switch—MS, three power transformers—PT, 750 MVA each, resistors—R, reactors—L. The measurement equipment for current measurements is—CM and voltage measurements—VM.

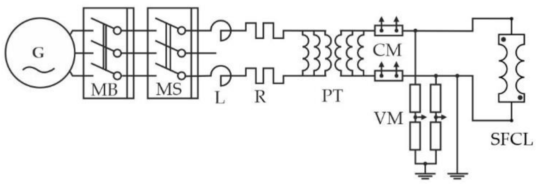

Scheme 1. A scheme of the circuit in the testing facility.

Figure 4. 2500 MVA short-circuit generator in Switchgear and Controlgear Testing Laboratory of Electrotechnical Institute in Warsaw.

3.1. Cooling the Limiter

It took 8 h to transport the limiter to the short circuit chamber of the testing facility, connect the busbars and vacuum pumps, and to install cryocooler. After obtaining a vacuum of the order of 10^{-3} mbar, a turbomolecular pump was launched. After 4 h of pumping, vacuum of about 10^{-6} mbar was obtained inside the cryostat, and good thermal insulation was achieved. The next step was to start the air-cooled helium compressor CSA71 (electrical power consumption max. = 7.2 kW) and cool down the SFCL. After 30 h of cooling, the limiter achieved 72 K.

3.2. Temperature Measurements

The temperature measurement of the SFCL windings is carried out with two LakeShore CERNOX CX-1070-AA-4L-QL cryogenic sensors calibrated to the 4 K–325 K range. The sensors are connected with phosphor bronze wires with a thermal conductivity much lower than that of copper. The sensors are connected to a LakeShore Monitor 218. One sensor is placed in the upper part of the windings and the other one in the lower part of the windings. Figure 5 shows the temperature readings during cooling and the difference between sensors readings. The temperature difference between the lower and the upper part of the windings is less than 2 K at 72 K during cooling. The temperature adjustment is an important advantage of conduction cooling; decreasing the windings temperature enables the HTS tape critical current to increase, and thus obtain the required parameters.

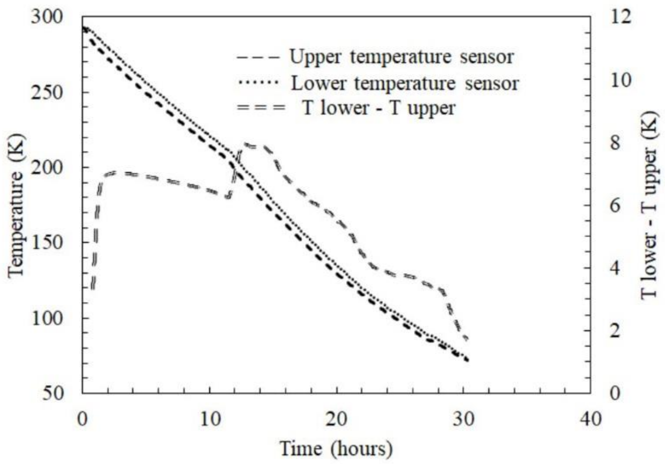

Figure 5. Temperature readings during cooling down and the difference between sensors readings.

3.3. Measurements of SFCL Parameters

The resistance of the SFCL, including the current leads, was 11.26 Ω at a room temperature and was 165 µΩ at cryogenic conditions. The inductance of the limiter was 3.32 µH. A very low inductance of the limiter in the superconducting state was achieved by good magnetic coupling of the superconducting windings. A high voltage test was carried out before and after. The insulation resistance between the SFCL terminals and grounded cryostat was more than 1 GΩ.

3.4. Fault Current Limiting Tests

Fault current limiting performance tests were conducted at 50 Hz. The tests were performed as a single phase short circuit to the ground. The RMS voltage value was set at 3.46 kV ($\approx$6 kV/$\sqrt{3}$). The short circuit time was set at 80 ms to protect the superconducting windings from overheating. The SFCL short circuit tests were preceded by fault current measurements in the circuit without the limiter.

4. Test Results

4.1. Limiting Performance

Figure 6 shows the voltage on the limiter and current courses during the first test at 72 K. The solid line indicates the current and the dotted line represents the voltage courses. As can be seen, the current was limited to 1.9 kA. The results of the second test performed at 80 K (Figure 7) show current limitation to the level of 1 kA. Both tests show excellent performance of the SFCL in reducing the fault current by more than 40 times (Figure 8).

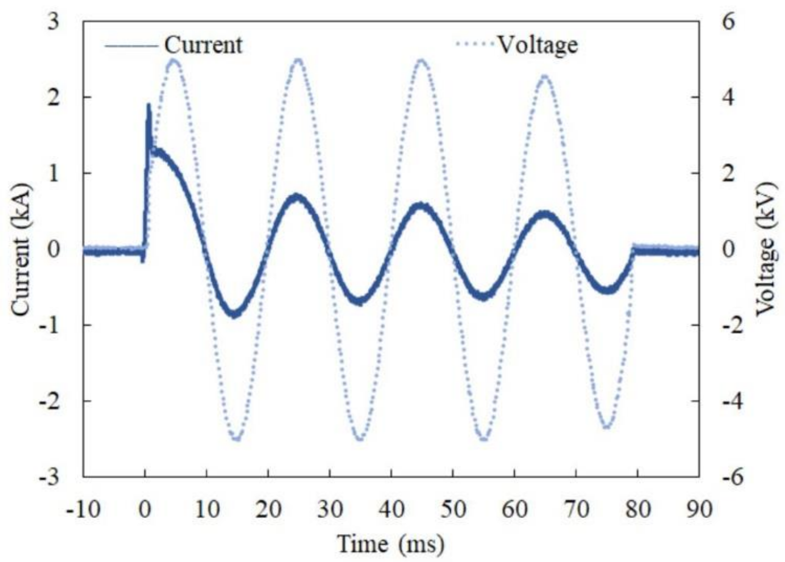

Figure 6. Voltage across the SFCL and current courses during short-circuit test at 72 K.

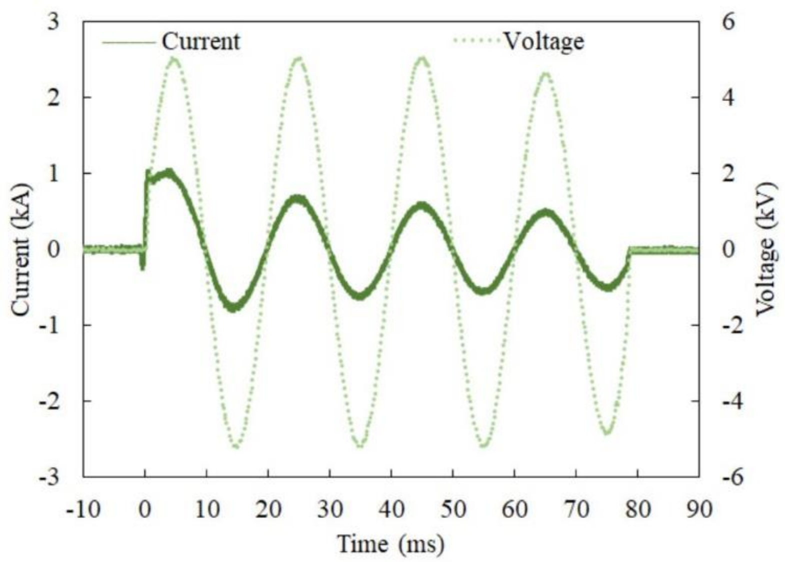

Figure 7. Voltage across the SFCL and current courses during short-circuit test at 80 K.

The limiter was tested at 72 K and at 80 K to compare the current in the circuit with the limiter to the current in the circuit without the limiter. In nominal conditions, the current passes through the compensated windings, and the voltage on the limiter is less than 0.2 V. During a short-circuit, the resistance of the superconducting windings increases. During a fault, the RMS voltage across the limiter was 3.4 kV (Figure 6). The maximum value of the surge current without the SFCL (limiter with shorted terminals) was 81 kA (Figure 8). After 80 ms of the short-circuit test, the temperature of the limiter windings increased by 5 K in the first 5 min and stabilized at 80 K after 10 min. The thermal capacity of the windings structure with copper plates allows for two tests to be carried out directly one after the other. A comparison of the SFCL current limiting effectiveness at 72 K and at 80 K is presented in Figure 9.

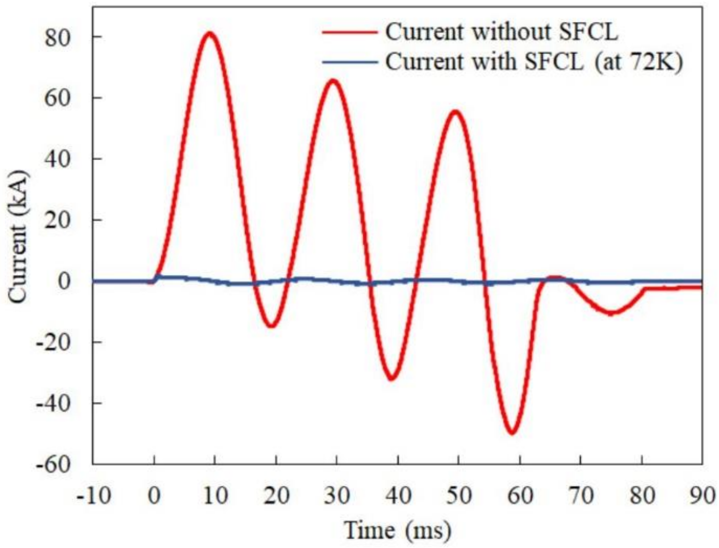

Figure 8. A comparison of current courses in the circuit with and without the limiter.

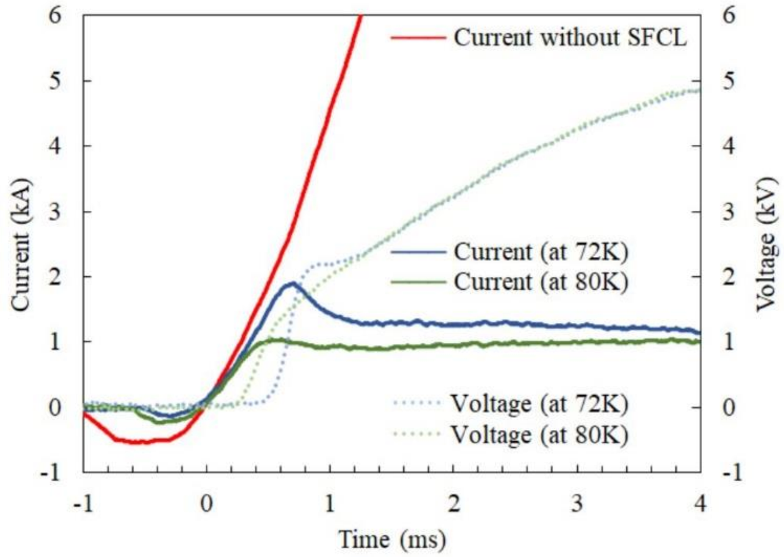

Figure 9. A comparison of current courses in the circuit without the limiter and with the limiter during the first 10 ms.

4.2. Response Time

In both tests, the response time of the surge current limitation is less than 1 ms. During the first test at 72 K, the peak value of the current occurs at about 0.6 ms after a fault. A rapid increase of the voltage on the limiter is observed after 0.4 to 0.8 ms after a fault. During the test at 80 K, a rapid increase in voltage occurs earlier (approx. 0.2 ms after the short-circuit) due to the drop in the critical current of the HTS tape at this temperature. Voltage courses start to overlap 1 ms after a fault. SFCL response time at both temperatures 72 K and 80 K is very fast—0.4 ms and 0.6 ms, respectively.

4.3. Limiter Resistance

The resistance of the limiter occurs very fast after a fault, limiting the surge value. A comparison of the limiter resistance development is presented on Figure 10. During the first 5 ms, the resistance value achieves more than 5 Ω and reaches about 10 Ω at the end of a fault after 80 ms. The resistance growth is significant at the beginning of a fault. The value of almost 2 Ω is reached within first millisecond.

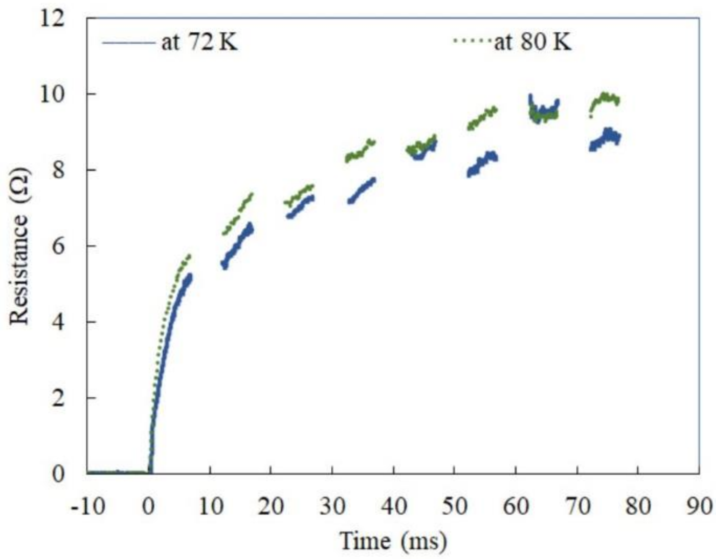

Figure 10. Comparison of SFCL resistance during fault at 72 K and at 80 K.

4.4. Power

The power generated in the limiter windings reached the highest value of about 5 MW after four milliseconds. The generated power caused the temperature of the HTS tape to increase rapidly. The temperature of the windings reached 160 K after 10 ms and 290 K after 80 ms of a fault.

5. Forces and Stresses

5.1. Forces Acting on Windings

During a short circuit, the limiter windings are subjected to a short-circuit current. The temperature of the windings increases from a cryogenic temperature to a room temperature. There are also forces acting on the windings. The direct cause behind the forces acting on the superconducting windings is the interaction of the magnetic field with the current HTS tape. In the case of an SFCL with push–pull windings, this is the leakage flux area. In normal operation, when the current in the windings does not exceed the critical current of the superconducting tape, the forces acting on the windings are small; whereas in case of short-circuits for currents much higher than the rated current, these forces can become dangerous for the superconducting windings. The forces acting on superconducting windings can be divided into radial and axial. Radial forces are the result of a field acting on the limiter windings in parallel to the winding axis (B_z component). The cause of the axial forces is a field perpendicular to the winding axis (B_r component) (Figure 11). From the distribution of the field and the direction of the current in the windings, it follows that axial forces act on the coils (Figure 12). With complete symmetry of the windings, the axial forces compress the turns of the outer winding and the inner winding. In the case of asymmetry, the direction and value of the forces can be determined from the magnetic flux density distribution calculated in the FEMM program (Figure 13). Axial forces resulting from spatial asymmetry of ampere-turns always tend to magnify it.

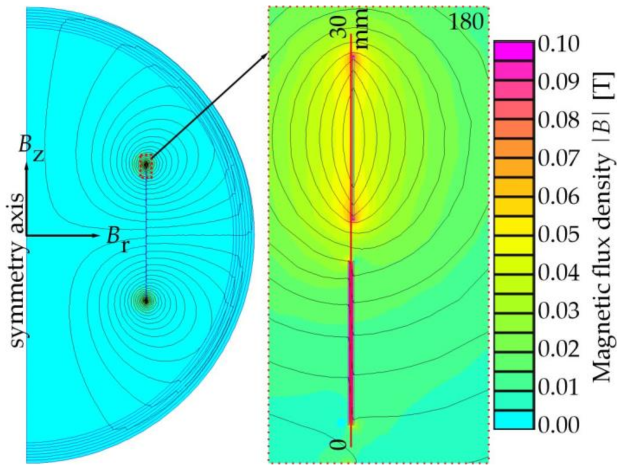

Figure 11. FEMM model of the SFCL windings, Red line 30 mm long between last turns is used to calculate axial and radial component of magnetic flux density.

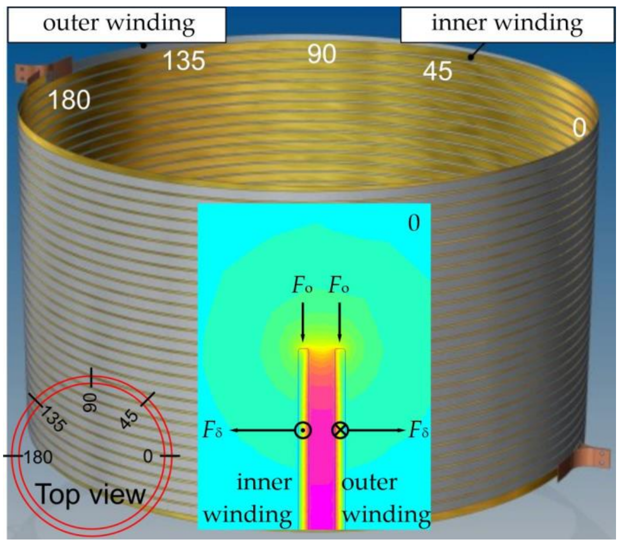

Figure 12. HTS windings of the SFCL.

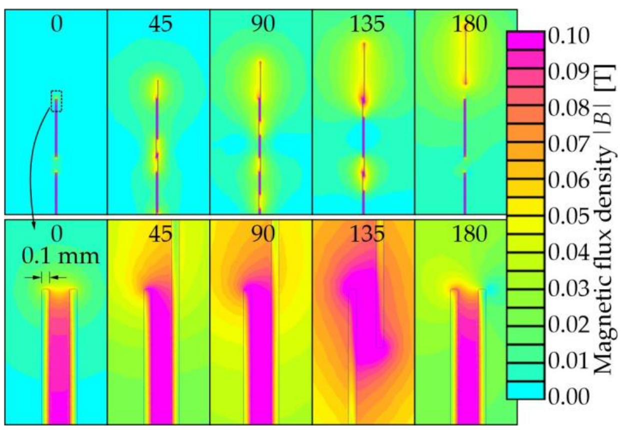

Figure 13. Magnetic flux density comparison at the angle 0 to 180 at the level of last turn.

The magnetic flux density varies with the location (Figure 14). The radial component of the magnetic flux density is shown on Figure 15. The axial component of the magnetic flux density calculated between windings is shown on Figure 16.

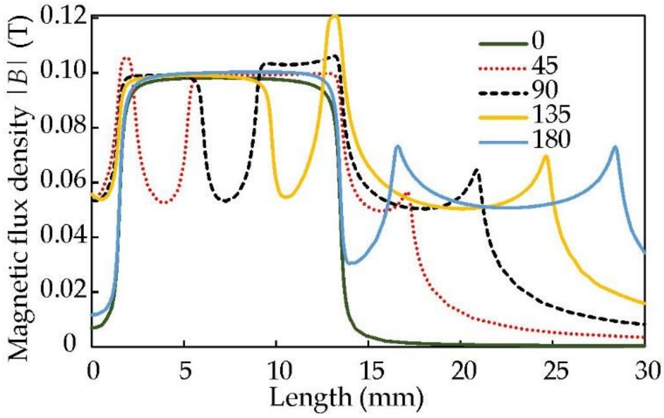

Figure 14. Magnetic flux density comparison at the angle 0 to 180 at the level of last turn between windings.

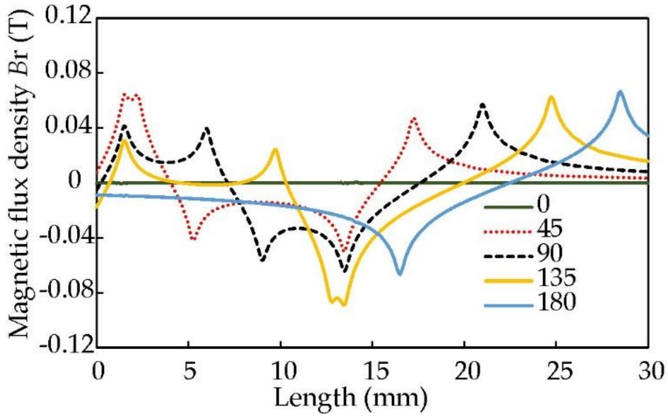

Figure 15. Magnetic flux density radial component.

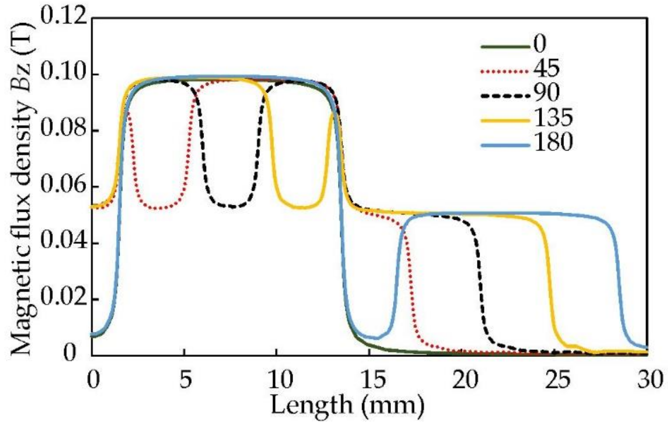

Figure 16. Magnetic flux density axial component.

5.2. Radial Forces

The radial forces affecting the windings during a short-circuit were limited by a special construction of the superconducting windings which are wound in opposite direction. Radial forces push the limiter windings apart. The winding design calculations were carried out under the assumption that the windings were perfectly rigid bodies. In reality, they have a certain elasticity. If a winding is wound tightly and has hard incompressible interlayer insulation, radial forces are transferred from the windings to the carcass. The highest stress in the conductor material occurs when the forces acting on the individual coils are not transmitted to the carcass. To calculate the radial forces acting on each coil, it is necessary to determine the axial component of the magnetic flux density. The value of the radial force for each coil also depends on its position in the winding. The axial component of the magnetic flux density (B_z) reaches its highest values around 0.1 T between the windings (Figure 13).

$$F_\delta = B_z I l_{turn}$$

where: B_z—axial component of magnetic flux density, I—current, l_{turn}—turn length.

The radial force determines the tensile force of the winding and the stress in the conductor (Figure 17).

$$F_r = \frac{F_\delta}{2\pi}$$

where: F_δ—radial force.

$$\sigma_r = \frac{F_r}{s}$$

where: F_r—tensile force, s—wire cross-section.

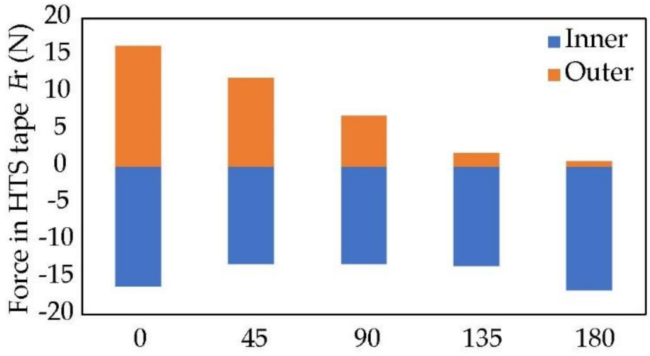

Figure 17. Tensile force in HTS tape during short-circuit.

The tensile force stresses the wires of the individual coils unevenly (Figure 18). When the winding is a completely rigid body, the individual coils are stressed only by their own forces, proportional to the magnetic flux density at the location determined by the position of the coil under consideration. The most stressed conductors are those located in the 0 degree position (Figure 12).

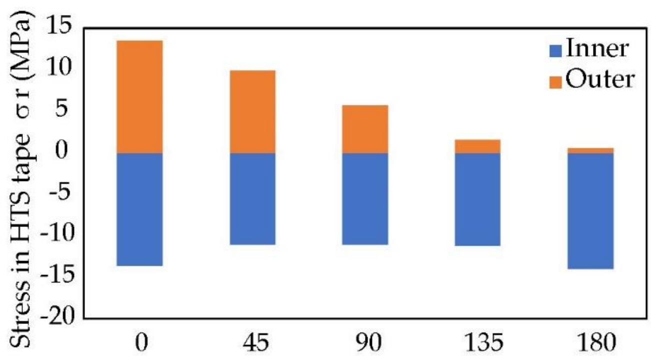

Figure 18. Stress in HTS tape during short-circuit.

The SuperPower® 2G HTS wire tolerates high stress up to 550 MPa. Above 550 MPa, I_c degrades irreversibly [40]. Presented limiter design assure safe operation assuring wire stress 40 times lower than maximum recommended value.

5.3. Axial Forces

The axial forces compress the turns of the outer winding and the inner winding at 0 degree (complete symmetry of the windings) (Figure 19).

$$F_o = B_r I l_{turn}$$

where: B_r—radial component of magnetic flux density, I—current, l_{turn}—turn length.

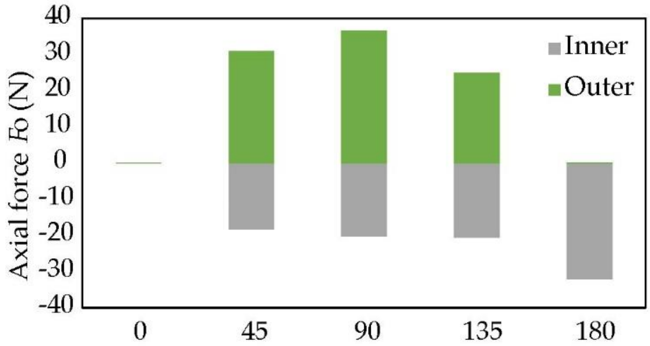

Figure 19. Axial force during short-circuit (upper turns).

In the case of asymmetry, the direction and value of the stress is determined from the magnetic flux density calculated in the FEMM (Figure 20). Axial forces resulting from spatial asymmetry of ampere-turns tend to magnify the asymmetry.

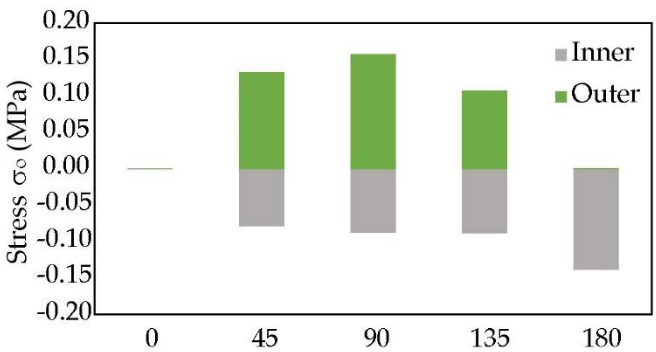

Figure 20. Stress during short-circuit (upper turns).

6. Conclusions

The concept of a compact, light and effective fault current limiter as a smart grid component has been realized. The superconducting resistive fault current limiter has been designed, manufactured and tested successfully in accredited Switchgear and Controlgear Testing Laboratory of Electrotechnical Institute in Warsaw.

The presented SFCL effectively limited the peak value of a fault current by more than 40 times (from 81 kA to 1.9 kA) within 0.6 ms. The maximum value of the short-circuit current measured during the limiter tests enabled accurate calculations of the stresses in the superconducting tape. The stress from axial force is below 0.15 MPa. The stress in the HTS wire resulting from radial force is 13.5 MPa, and is much lower than the recommended maximum value (550 MPa). The applied solution of a conduction-cooled SFCL with compensated superconducting windings which are connected in parallel substantially limited the voltage in the limiter, making the limiter invisible to the grid at working currents. The thermal capacity of the windings structure allows the windings to rapidly return to the superconducting state after a short-circuit. The conduction cooling method simplifies the cryogenic system to the degree which allows the limiter to be installed next to a circuit breaker. The absence of a liquid nitrogen installation reduces the size and the cost of the system, and increases the reliability of the limiter cooling. The conduction cooling method using a cryocooler also offers a substantial advantage over liquid nitrogen bath cooling: by changing the temperature, the critical current of the HTS tape can be adjusted easily. Further, any adjustments to the parameters can be made remotely by setting the SFCL temperature in order to dovetail them to the smart grid expectations The presented results of calculations of forces and stresses acting on the HTS tape which the limiter windings are made of allow us to conclude that the presented design of the limiter windings ensures its safe operation during limiting of short-circuit currents. The stress values are significantly lower than the maximum values and do not cause irreversible degradation of the superconducting windings.

Funding: This work was supported in part by the National Fund for Environmental Protection and Water Management and The National Centre for Research and Development under Grant GEKON2/O2/267193/13/2015, and by the Lublin University of Technology under Grant FD-20/EE-2/408.

Institutional Review Board Statement: Not applicable.

Informed Consent Statement: Not applicable.

Data Availability Statement: Not applicable.

Conflicts of Interest: The author declare no conflict of interest.

References

1. Kozak, J.; Majka, M.; Kozak, S. Experimental Results of a 15 kV, 140 A Superconducting Fault Current Limiter. *IEEE Trans. Appl. Supercond.* **2017**, *27*, 5600504. [CrossRef]
2. Kozak, J.; Majka, M.; Blazejczyk, T.; Berowski, P. Tests of the 15-kV Class Coreless Superconducting Fault Current Limiter. *IEEE Trans. Appl. Supercond.* **2016**, *26*, 5600804. [CrossRef]
3. Majka, M.; Kozak, J.; Kozak, S.; Wojtasiewicz, G.; Janowski, T. Design and Numerical Analysis of the 15 kV Class Coreless Inductive Type SFCL. *IEEE Trans. Appl. Supercond.* **2014**, *25*, 5601005. [CrossRef]
4. Kozak, J.; Majka, M.; Janowski, T.; Kozak, S.; Wojtasiewicz, G.; Kondratowicz-Kucewicz, B. Tests and Performance Analysis of Coreless Inductive HTS Fault Current Limiters. *IEEE Trans. Appl. Supercond.* **2011**, *21*, 1303–1306. [CrossRef]
5. Naeckel, O.; Noe, M. Design and Test of an Air Coil Superconducting Fault Current Limiter Demonstrator. *IEEE Trans. Appl. Supercond.* **2013**, *24*, 5601605. [CrossRef]
6. Kado, H.; Ickikawa, M. Performance of a high-Tc superconducting fault current limiter-design of a 6.6 kV magnetic shielding type superconducting fault current limiter. *IEEE Trans. Appl. Supercond.* **1997**, *7*, 993–996. [CrossRef]
7. Heydari, H.; Abrishami, A.A.; Bidgoli, M.M. Comprehensive Analysis for Magnetic Shield Superconducting Fault Current Limiters. *IEEE Trans. Appl. Supercond.* **2013**, *23*, 5604610. [CrossRef]
8. Nackel, O.; Noe, M. Conceptual Design Study of an Air Coil Fault Current Limiter. *IEEE Trans. Appl. Supercond.* **2012**, *23*, 5602404. [CrossRef]
9. Heydari, H.; Sharifi, R. Three-Dimensional Pareto-Optimal Design of Inductive Superconducting Fault Current Limiters. *IEEE Trans. Appl. Supercond.* **2010**, *20*, 2301–2311. [CrossRef]
10. Sharifi, R.; Heydari, H. Viable Inductive Superconducting Fault-Current Limiters Using Autotransformer-Based Hybrid Schemes. *IEEE Trans. Appl. Supercond.* **2011**, *21*, 3514–3522. [CrossRef]
11. Jingye, Z.; Dai, S.; Wang, Z.; Zhang, D.; Zhang, Z.; Zhang, F.; Xu, Z.; Zhu, Z.; Zhang, G.; Xu, X.; et al. Design, fabrication, and tests of three HTS coils for a model fault current limiter. *IEEE Trans. Appl. Super-Cond.* **2010**, *20*, 1135–1138. [CrossRef]
12. Kozak, J.; Majka, M.; Kozak, S.; Janowski, T. Design and Tests of Coreless Inductive Superconducting Fault Current Limiter. *IEEE Trans. Appl. Supercond.* **2012**, *22*, 5601804. [CrossRef]
13. Hekmati, A.; Hosseini, M.; Vakilian, M.; Fardmanesh, M. A novel method of flat YBCO rings development for shield-type superconducting fault current limiters fabrication. *Phys. C Supercond.* **2012**, *472*, 39–43. [CrossRef]
14. Kvitkovic, J.; Pamidi, S.V.; Graber, L.; Chiocchio, T.; Steurer, M.; Usoskin, A. AC loss and magnetic shielding measurements on 2G HTS inductive fault current limiter prototype modules. *IEEE Trans. Appl. Supercond.* **2014**, *24*, 5600604. [CrossRef]
15. de Sousa, W.T.B.; Nackel, O.; Noe, M. Transient Simulations of an Air-Coil SFCL. *IEEE Trans. Appl. Supercond.* **2014**, *24*, 5601807. [CrossRef]
16. Kozak, J.; Majka, M.; Janowski, T.; Kozak, S. Superconducting coreless inductive fault current limiter for medium-voltage systems. *Prz. Elektrotech.* **2012**, *88*, 245–248.
17. Kozak, J.; Majka, M.; Janowski, T.; Kozak, S. Design and Development of the First Polish Superconducting Fault Current Limiter For MV Distribution Systems. *Phys. Procedia* **2012**, *36*, 845–848. [CrossRef]

18. Majka, M.; Kozak, J.; Janowski, T.; Kozak, S. Performance analysis of coreless inductive superconducting fault current limiters made of the first and second generation HTS tape. *Prz. Elektrotech.* **2012**, *88*, 32–35.
19. Li, B.; Wang, C.; Wei, Z.; Xin, Y.; Li, B.; He, J. Technical Requirements of the DC Superconducting Fault Current Limiter. *IEEE Trans. Appl. Supercond.* **2018**, *28*, 5602805. [CrossRef]
20. Hong, H.; Su, B.; Niu, G.J.; Cui, J.B.; Tian, B.; Li, Q.; Wang, L.Z.; Wang, Z.H.; Zhang, K.; Xin, Y. Design, fabrication, and operation of the cryogenic system for a 220 kV/300 MVA saturated iron-core su-perconducting fault current limiter. *IEEE Trans. Appl. Supercond.* **2014**, *24*, 9002204. [CrossRef]
21. Li, B.; Jing, F.; Li, B.; Chen, X.; Jia, J. Study of the Application of Active Saturated Iron-Core Superconductive Fault Current Limiters in the VSC-HVDC System. *IEEE Trans. Appl. Supercond.* **2018**, *28*, 5602906. [CrossRef]
22. Ma, T.; Dai, S.; Song, M.; Li, C. Electromagnetic Design of High-Temperature Superconducting DC Bias Winding for Single-Phase 500 kV Saturated Iron-Core Fault Current Limiter. *IEEE Trans. Appl. Supercond.* **2017**, *28*, 5200805. [CrossRef]
23. Noe, M.; Hobl, A.; Tixador, P.; Martini, L.; Dutoit, B. Conceptual Design of a 24 kV, 1 kA Resistive Superconducting Fault Current Limiter. *IEEE Trans. Appl. Supercond.* **2011**, *22*, 5600304. [CrossRef]
24. Yan, S.; Tang, Y.; Ren, L.; Xu, Y.; Wang, Z.; Liang, S.; Zhang, Z. Design and Verification Test of a Flux-Coupling-Type Superconducting Fault Current Limiter. *IEEE Trans. Magn.* **2018**, *24*, 9000105. [CrossRef]
25. Han, T.-H.; Ko, S.-C.; Lim, S.-H.; Ko, S.-C. Fault Current Limiting Characteristics of Transformer-Type Superconducting Fault Current Limiter Due to Winding Direction of Additional Circuit. *IEEE Trans. Appl. Supercond.* **2018**, *28*, 5601906. [CrossRef]
26. Kozak, J.; Majka, M.; Kozak, S.; Janowski, T. Comparison of Inductive and Resistive SFCL. *IEEE Trans. Appl. Supercond.* **2012**, *23*, 5600604. [CrossRef]
27. Didier, G.; Bonnard, C.; Lubin, T.; Lévêque, J. Comparison between inductive and resistive SFCL in terms of current limitation and power system transient stability. *Electr. Power Syst. Res.* **2015**, *125*, 150–158. [CrossRef]
28. Morandi, A. State of the art of superconducting fault current limiters and their application to the electric power system. *Phys. C Supercond.* **2013**, *484*, 242–247. [CrossRef]
29. Kempski, A.; Rusinski, J. A study of the Superconducting Fault Current Limiter application in a MV network with distributed energy sources. In Proceedings of the 2017 Progress in Applied Electrical Engineering (PAEE), Koscielisko, Poland, 25–30 June 2017.
30. Rebizant, W.; Solak, K.; Brusilowicz, B.; Benysek, G.; Kempski, A.; Rusiński, J. Coordination of overcurrent protection relays in networks with superconducting fault current limiters. *Int. J. Electr. Power Energy Syst.* **2018**, *95*, 307–314. [CrossRef]
31. Hayakawa, N.; Maeno, Y.; Kojima, H. Fault Current Limitation Coordination in Electric Power Grid with Superconducting Fault Current Limiters. *IEEE Trans. Appl. Supercond.* **2018**, *28*, 5602304. [CrossRef]
32. Rusiński, J. Impact of superconducting fault current limiter on the distributed energy source work. *IET Gener. Transm. Distrib.* **2017**, *12*, 310–317. [CrossRef]
33. Olejnik, B. Adaptive Zero-Sequence Overcurrent Criterion for Earth Fault Detection for Fault Current Passage Indicators in Resistor Grounded Medium Voltage Networks. *IEEE Access* **2021**, *9*, 63952–63965. [CrossRef]
34. Xu, Z.; Li, X.; Stojanovic, V. Exponential stability of nonlinear state-dependent delayed impulsive systems with appli-cations. *Nonlinear Anal. Hybrid Syst.* **2021**, *42*, 101088. [CrossRef]
35. Zhang, X.; Wang, H.; Stojanovic, V.; Cheng, P.; He, S.; Luan, X.; Liu, F. Asynchronous Fault Detection for Interval Type-2 Fuzzy Nonhomogeneous Higher Level Markov Jump Systems With Uncertain Transition Probabilities. *IEEE Trans. Fuzzy Syst.* **2021**, *30*, 2487–2499. [CrossRef]
36. Tsotsopoulou, E.; Karagiannis, X.; Papadopoulos, P.; Dysko, A.; Yazdani-Asrami, M.; Booth, C.; Tzelepis, D. Time-Domain Protection of Superconducting Cables Based on Artificial Intelligence Classifiers. *IEEE Access* **2022**, *10*, 10124–10138. [CrossRef]
37. García, G.; Marene Larruskain, D.; Etxegarai, A. Modelling of Resistive Type Superconducting Fault Current Limiter for HVDC Grids. *Energies* **2022**, *15*, 4605. [CrossRef]
38. Kozak, J.; Majka, M.; Kozak, S. Design Considerations on a Resistive Superconducting Fault Current Limiter. *Acta Phys. Pol. A* **2020**, *138*, 710–714. [CrossRef]
39. Kozak, S. Superconducting Surge Current Limiter. *Energies* **2021**, *14*, 6944. [CrossRef]
40. Data from Superpower Inc. Available online: https://superpower-inc.com (accessed on 30 July 2022).